JOURNAL OF MATERIALS SCIENCE **34** (1999) 5403–5406

Laser sintering of Cu-Sn-C system P/M alloys

GUO ZUOXING, HU JIANDONG, ZHOU ZHENFENG
Microanalysis Center, Jilin University of Technology, Changchun, 130025, People's Republic of China

The Cu-Sn-C system P/M alloys were sintered by laser. The influence of laser sintering on the properties of the laser-sintered materials was investigated. The properties, such as the density, impact toughness, hardness and wear resistance of the laser-sintered materials are desirable. A maximum impact toughness of 11.7 J/cm^2 was achieved and the wear resistance of the laser-sintered materials was tremendously increased compared with conventional sintering. The green compact made from Cu-Sn-C powders, with a thickness of 10 mm, can be penetratively sintered by using a suitable processing condition. The laser sintering was characterised by a thermal cycle which was accomplished in a relatively short time, resulting in a relatively high temperature (950 °C). The curves showing temperature profiles for the top surface and bottom of the laser-sintered specimen were recorded by thermocouples. Differences in temperatures between the top surface and bottom were very small, less than 60 °C. Some intermetallics/phases such as α-Cu, $Cu_{31}Sn_8(\delta)$, $Cu_3Sn(\varepsilon)$ and $Cu_6Sn_5(\eta)$ were most readily produced in the laser-sintered materials and their distributions were more homogeneous than conventional sintering, owing to the better flow ability of the melt caused by a relatively high sintering temperature. The behaviour of diffusion between Cu and Sn was also studied by means of simulation diffusion couple.

1. Introduction

Cu-Sn alloys have most widely been used as self-lubricating materials for many years [1, 2], and powder metallurgy has been a main process to fabricate the alloys. Some components which undergo wear in practical situation should have much less wear for their friction couple. For example, pantograph/collector, which is used for collecting electrical current from the overhead cable of electric trains, is a typical of component requiring less wear to the electrical cable largely because of its expensive cost. Cu-Sn-C system alloy is a good candidate for this purpose. Since the miscibility of C in the Cu-Sn alloy is very poor, it is difficult to sinter Cu-Sn-C P/M alloys to become a high strength alloy. In the present study, green compact laser sintering (GCLS) which can produce a high density P/M structural part [3–5], will be adopted to sinter the Cu-Sn-C powder materials. The purpose of this paper is to study the properties and microstructures of the laser-sintered Cu-Sn-C system P/M alloys. The characteristic of the GCLS is also discussed in the paper.

2. Experimental

The powders used for experiments were copper, tin and graphite with a size of range from −250 to −300 mesh. The compositions of the powder mixtures are listed in Table I.

The various powders were mixed in a self-made mixing machine. With the powder mixtures of 500 g load, the machine was operated at a speed of 30 rpm for 3.5 h. After the homogeneity was confirmed by chemical analysis, the mixtures were then compacted into specimens at a pressure of 400 MPa, producing the green compact with a size of $10 \times 10 \times 55$ mm. A 2kW CO_2 laser generator was employed to sinter the green compacts using a beam size of 30 mm in diameter and a scanning rate of range in 0–20 mm/min. Thermocouples connected to an automatic x-y recorder were used to monitor temperature profiles during laser sintering. For the purpose, two small holes with a depth of 1 mm were carefully drilled on the top surface and bottom of the specimen, and the ends of the thermocouples were then mounted in the holes. Consequently, two temperature curves can be obtained at the same time. The density of the sintered specimens was calculated through an equation of density = weight/volume. The size of the specimens used for wear test is $10 \times 10 \times 14$ mm. A sample-on-the-wheel reciprocation wear test machine was used. The specimens were clamped to the wear test machine. A friction wheel made of copper was employed as a friction couple to wear the sintered materials. The friction wheel was run at a speed of 400 rpm under an applied load of 10 kg, and wear time was 30 min for each friction couple, under an unlubrication condition. A balance with an accuracy of 0.1 mg was used to determine the weight loss for each worn specimen and copper wheel. The morphology of the worn surface was observed by SEM and compositions in the laser sintered specimens were examined by EDS.

TABLE I Composition of powder mixtures (wt %)

No.	1	2	3	4	5	6	7	8	9	10
Cu	bal.	bal.	bal.	bal.	bal.	bal.	bal.	bal.	bal.	bal.
Sn	3	3	3	3	3	2	3	4	5	6
C	2	3	4	5	6	6	6	6	6	6

TABLE II Properties of specimens laser sintered

	Density (g/cm^3)	Hardness HRB	Impact (J/cm^2)	Weight loss of specimen (mg)	Weight loss of friction wheel (mg)
GCLS	6.07	38	5.78	1.7	5.0

X-ray diffraction test was carried out on a D/max-rA type diffractometer using Cu target and graphite filter.

3. Results and discussion

3.1. Influence of C content on properties

For the laser-sintered specimens, the properties change as C content increases; as shown in Fig. 1 and Fig. 2.

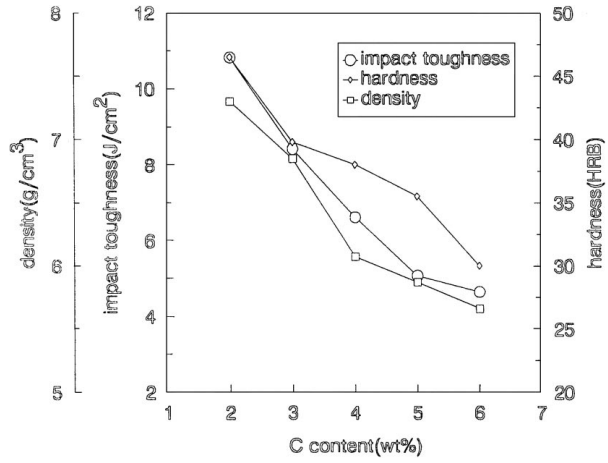

Figure 1 Variations of properties with C content (3 wt %Sn).

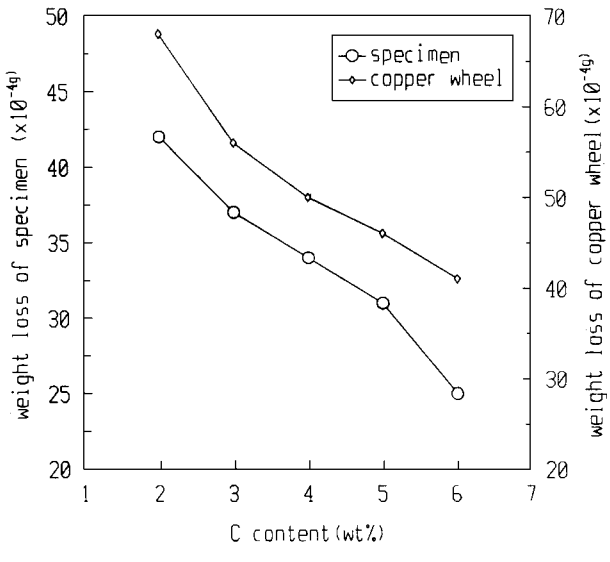

Figure 2 Variations of wear resistance with C content (3 wt %Sn).

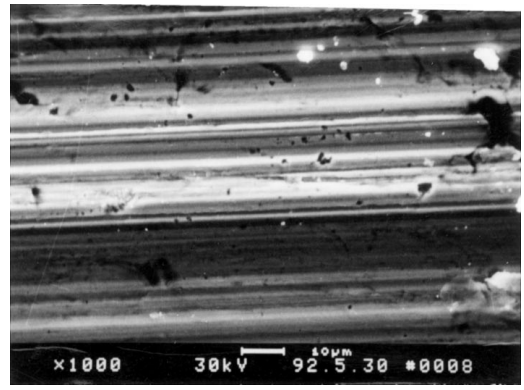

Figure 3 SEM photograph, showing morphology of worn surface for the laser-sintered specimens.

The density, impact toughness, and hardness of the laser-sintered materials all decrease with increasing C content, especially for the impact toughness which has a maximum value of 11.7 J/cm^2 at 2%C and a minimum value of 4.3 J/cm^2 at 6%C. Thus, the effect of C content on the impact toughness is much more obvious. The characteristics of wear resistance for both the specimens and the friction wheel are reflected in Fig. 2, showing the weight loss variations with C content. The weight loss of the specimens and friction wheel decreases with increasing C content, indicating that the self-lubricating effect of the graphite in the laser-sintered specimen is well utilized. The wear resistance of the laser-sintered specimen is very good. (see Table II). In order to investigate the reason for the enhanced wear resistance, SEM was used to observe the worn surfaces. The ploughed ditches of the worn surface in the laser-sintered are not only shallow but also narrow (see Fig. 3). It was observed by SEM that almost all the graphite were firmly attached to the matrix in the laser-sintered materials, leading to the better wear resistance. Therefore, it is concluded that the lubrication effect of the graphite on the wear resistance could be dominant in the laser-sintered condition.

3.2. Influence of Sn content on properties

Fig. 4 shows the density, impact toughness and hardness variations with Sn content for the laser sintered specimens. Almost all the properties significantly increase with increasing Sn content, showing there is a big influence of Sn content on the density, impact toughness and hardness increase. Amounts of intermetallics/phases formed in the Cu-Sn alloy increase as Sn content increases. Thus, it is thought that the enhanced hardness, density and impact toughness are attributed to the formation of the intermetallcs/phases because of their high hardness. For the wear resistance (see Fig. 5), the

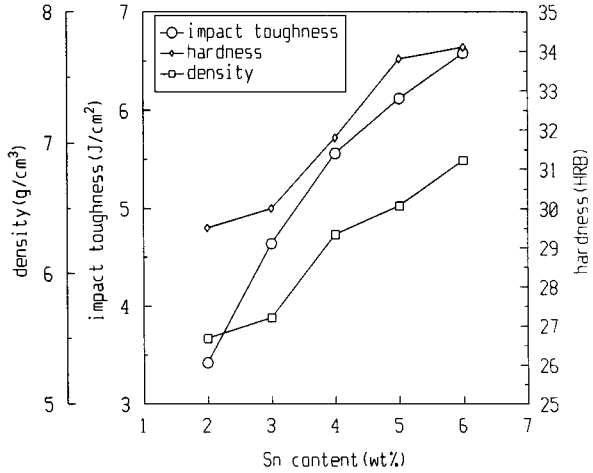

Figure 4 Variations of properties with Sn content (6 wt %C).

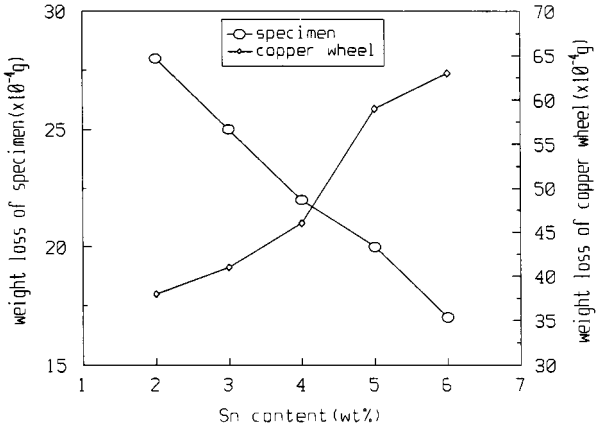

Figure 5 Variations of wear resistance with Sn content (6 wt %C).

weight loss of the specimens decreases with increasing Sn content. Conversely, the weight loss of Cu friction wheel increases with increasing Sn content. It is because the hardness values of the laser-sintered materials are much higher than that of those Cu friction wheels. The properties of the laser sintered specimens are shown in Table II.

3.3. Microstructure

Fig. 6 shows morphology for the laser-sintered specimen. The microstructure includes α-Cu, graphite as well as some precipitates. The α-Cu phases are characterized by twinning structure. As can be seen, the graphite is well combined with the matrix. It is difficult to find pores by microstructure observation, but the porosities were calculated to be 10–15% for the laser-sintered materials.

3.4. Temperature profile

Two curves indecating temperature variations with time for both the top surface and bottom of the laser-sintered specimen are given in Fig. 7. As can be seen, each curve is characterized by a typical thermal cycle. The thermal cycle consists of heating and cooling, and the former of which is accomplished in less than 70 s. The curves show a maximum temperature value of 950 °C for the

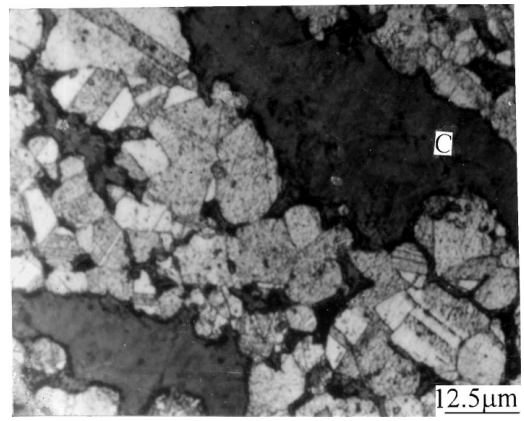

Figure 6 Optical photograph, showing microstructure for laser-sintered specimen, etched with a solution of $FeCl_3$(5 g), HCl(2 ml) and ethanol (96 ml).

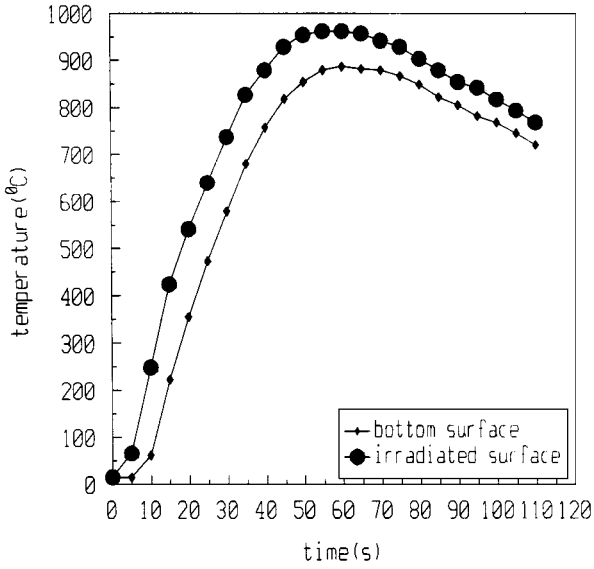

Figure 7 Temperature vs time.

top surface(irradiated surface) and 890 °C for the bottom. Starting time for the bottom being heated is later than that for the top surface and the difference is about 5 s, as shown in Fig. 7. The maximum temperature values for the top surface and bottom are different, but they reach their maximum values at almost the same time. The higher sintering temperature and shorter sintering cycle of laser sintering result in a liquid phase sintering mechanism.

The hardness values of both the top surface and bottom were examined, and the results are shown in Table III. The numbers are representative of the measured points on the laser-sintered specimens. There are no significant differences in hardness values for them. Thus, it is likely that the differences in the temperatures make no significant microstructure changes.

TABLE III Hardness of top surface and bottom (HRB)

	1	2	3	4
Top sur.	37.5	39.0	37.0	38.0
Bottom	36.8	39.2	38.2	37.7

3.5. Diffusion of Cu and Sn during laser sintering

In order to investigate composition distribution in the laser-sintered specimen, a diffusion couple consisting of Cu and Sn was employed to simulate diffusion between Cu and Sn (see Fig. 8). After the diffusion couple was irradiation for 10 s, the compositions of which in various positions were detected by EDS. Curves in Fig. 9 show Cu and Sn content variations with distance and the interface of the original Cu and Sn regions is marked with number 6 (see Fig. 8). It is clear that there is a drastic increase in Cu in the original Sn region, being up to 50%. In contrast, Sn in the original Cu region is relatively less. This indicates that Cu atoms diffuse into Sn rapidly. The transformed products on heating and cooling are very complex, but Sn melting must have occurred due to its lower melting point and a high sintering temperature. Consequently, the melts can flow along the gaps between the graphite and the other particles and form some solidified structures around the graphite on cooling. It is likely that the graphite closely associated with the solidified structures may be well combined with the matrix. On the other hand, the melt may leave pores during laser sintering and this can provide chances for Cu and graphite particles to be rearranged, resulting in the densitized materials. The solid state diffusion may also occur prior to melting, but main densification mechanism for the GCLS is liquid sintering. In this case, solid state diffusion, evaporation as well as condensation are all possible phenomena. As measured by the X-ray diffractometer, the laser sintered structures contained many intermetallics/phases. Some of them are calculated to be α-Cu, $Cu_{31}Sn_8(\delta)$ $Cu_6Sn_5(\eta)$ and $Cu_3Sn(\varepsilon)$.

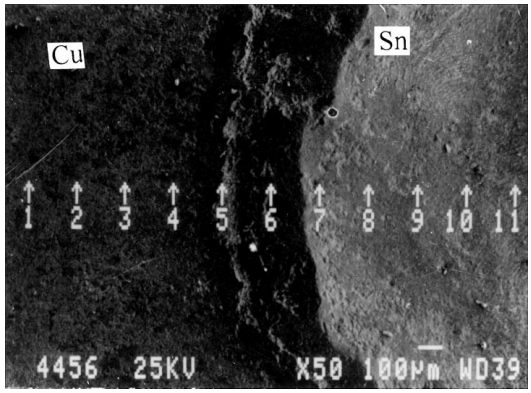

Figure 8 SEM photograph, which shows a Cu and Sn diffusion couple. Original Cu region and Sn are labeled with letter Cu and Sn, respectively. Short arrows in photograph are representative of points to be measured.

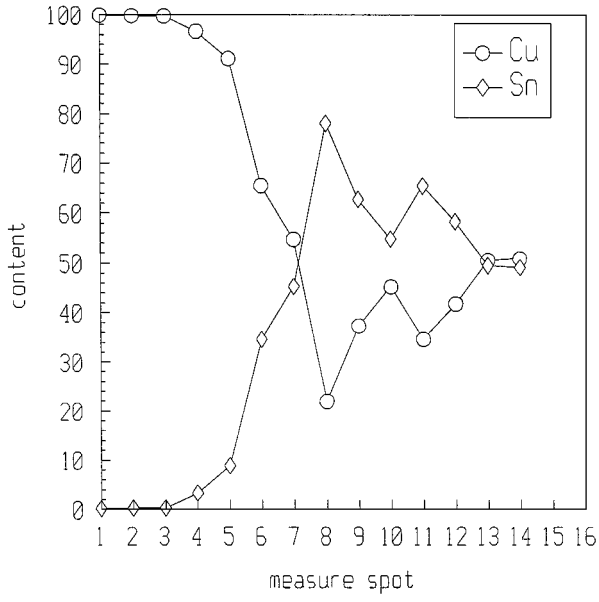

Figure 9 Variation of Cu and Sn contents with distance, showing composition distribution in a diffusion couple, cross point is located in the original interface between Cu and Sn.

4. Conclusion

Cu-Sn-C system P/M alloys were successfully fabricated by the GCLS. The laser sintering was characterized by a thermal cycle, allowing relatively high sintering temperature. Specimen with a size of $10 \times 10 \times 55$ mm can be penetratively sintered. The laser-sintered specimens included many intermetallics/phases such as α-Cu, $Cu_{31}Sn_8(\delta)$, $Cu_6Sn_5(\eta)$ and $Cu_3Sn(\varepsilon)$, which were homogeneously distributed. In comparison with the conventional sintering, the laser sintering produced the better properties to the laser-sintered specimen. The wear resistance of the laser-sintered specimen is very good. A maximum impact toughness value of 11.7 J/cm^2 was achieved. Cu diffusion in Sn was very fast. The enhanced density for the laser-sintered specimens is attributed to the liquid phase sintering mechanism, resulting from high temperatures. The fact that the properties such as the density, hardness, impact toughness and wear resistance of the laser-sintered specimens were much better than those conventionally sintered indicates that GCLS is a potential process for the sintering of P/M parts and could be applied in the field of Rapid Prototping or P/M.

Acknowledgements

The authors would like to thank Dr. Shen Ping for many fruitful discussions.

References

1. NARENDRA N. ACHARGA and PUDUKOTTAH G. MUKUNDA, *The International Journal of Powder Metallurgy* **31** (1995) 63.
2. J. W. KIM, S. J. L. KANG and D. N. YOON, *Powder Metallurgy International* **19** (1987) 41.
3. HU JIANDONG and LI ZHANG, in "Invention Patent Bulletin," edited by Chinese National Patent Bureau (Beijing, China, 1992) p. 15.
4. HU JIANDONG, LI YULONG, LI ZHANG, BU XIANZHANG and WANG LICHUN, *J. Mater. Sci.* **28** (1993) 796.
5. HU JIANDONG, GUO ZOUXING GUAN QINGFENG and LI YULONG, *Optics and Laser Technology* **29** (1997) 75.

Received 10 March 1997
and accepted 3 March 1999